

## Supplementary Material

### *Clinical information of patients with the variant in the PPARA gene*

#### *Patient A [PPARA c.209-2delA (exon4 skipping)]*

Patient A was a Japanese female with paranoid schizophrenia harboring a heterozygous mutation (c.209-2delA) in the *PPARA* gene. The patient grew up at an infant home until the age of 2 years and 9 months. During childhood, the patient grew up at a foster home or a childcare house. The patient attended general elementary, junior high, and high schools. At the age of 19 years, the patient was diagnosed with schizophrenia by a psychiatrist. At the age of 25, the patient was housed at the Women's Center and admitted to a hospital. At the age of 28 years, the patient was admitted to the hospital again. After discharge from the hospital, the patient continued to receive outpatient care. At the study evaluation time period, the patient was 34 years of age. The details of patient disease progress, drug therapy, and familial history of psychiatric illness were unavailable. The blood biochemical scores of the patient related to lipid metabolism were within the normal range.

#### *Patient B [PPARA (His117Gln)]*

Patient B was a Japanese female with residual schizophrenia harboring a heterozygous missense mutation (His117Gln) in the *PPARA* gene. Placental abruption was observed at birth. At 1 year of age, the growth of the patient was insufficient. At 4 years of age, the patient was diagnosed with a stutter and received support for the language development disorder related to stuttering. The patient attended elementary, junior high, and high schools. The patient performed poorly in tests in junior high and high schools. Although the patient temporarily refused to go to school during high school, the patient graduated from high school. After graduation from a technical school, the patient did not find a job and lived at home.

At the age of 20, the patient was diagnosed with schizophrenia and was treated with psychotropic drugs. The drug treatment stabilized the psychiatric symptoms of the patient. The patient worked several jobs and was working during the study period. The patient had no history of psychiatric hospitalization, and the blood biochemical scores related to lipid metabolism were within the normal range. At the study evaluation point, the patient was 34 years old. The patient's mother was diagnosed with dysthymia, while a maternal uncle was admitted to a psychiatric hospital for a long time. The details of the familial history of psychiatric illness were unavailable.

*Patient C [PPARA (Arg141Cys)]*

Patient C was a Japanese male with residual schizophrenia harboring a heterozygous missense mutation (Arg141Cys) in the *PPARA* gene. At the age of 27 years, the patient was diagnosed with schizophrenia. At the study evaluation time point, the patient was 64-year-old and was on an antipsychotic treatment regime of 200 mg/day quetiapine, 20 mg/day olanzapine, and two macrolide antibiotic tablets/day. The details related to patient disease progress, drug therapy, and familial history of psychiatric illness were unavailable.

*Patient D [PPARA (Arg226Trp)]*

Patient D was a Japanese male with residual schizophrenia and harbored a heterozygous missense mutation (Arg226Trp) in the *PPARA* gene. The patient was diagnosed with schizophrenia at the age of 19 years. At the study evaluation time point, 52-year-old. The details of the patient disease process, drug therapy, and familial history of psychiatric illness were unavailable.

Consent for publication was obtained from the four patients.

## Supplementary Materials and Methods

### *Targeted next-generation sequencing (NGS) using molecular inversion probes (MIP)*

A 15- $\mu$ L reaction volume comprising 50 ng genomic DNA, 250 fmol of 5' - phosphorylated MIPs mixture, 1.5  $\mu$ L of 10X Ampligase DNA ligase buffer (Epicentre Biotechnologies, Madison, WI, USA), 0.3  $\mu$ M dNTP (Invitrogen, Carlsbad, CA, USA), 0.2  $\mu$ L Hemo KlenTaq (New England Biolabs, NEB, Ipswich, MA, USA), and 1 U Ampligase (Epicentre Biotechnologies) was prepared in molecular biology grade water. The samples were subjected to denaturation at 95 °C for 10 min and incubated at 60 °C for 22 hours. The linear probes and the remaining genomic DNA were removed by exonuclease treatment. Next, the sample was subjected to PCR amplification using the barcoded reverse primers. Initially, 48 PCR products were pooled, purified, and sequenced using an Illumina MiSeq (Illumina, San Diego, CA, USA) platform with 150-bp paired-end runs. The same method was employed to pool, purify, and sequence 384 PCR products using a rebalanced MIP-mixture and Illumina HiSeq2000 (Illumina) Rapid mode 150-bp paired-end runs.

In accordance with the Genome Analysis ToolKit (GATK) best practices [1], the raw reads were mapped to the genome (GRCh37 build) using Burrows-Wheeler Aligner (BWA MEM) (0.7.5a-r405), and the data were converted to .bam files using Picard-tools (1.137). The GATK (3.4-46) tool was used for indel realignment, base-quality recalibration, and variant discovery. Individual variant calling was performed with the GATK Haplotype Caller, followed by multi-sample genotyping. The variants were then hard filtered. Variants with quality score (QUAL) < 30.0, quality by depth (QD) < 5.0, genotype quality (GQ) < 20.0, heterozygous allele balance (ABHet) > 0.75, and homopolymer run (HRun)  $\geq$  4, and clustered variants were excluded from the analysis. The variants were filtered to identify the missense and loss-of-function (LoF) variants (stop gained, stop lost, start lost, and

variants at the splice donor and acceptor sites). The genetic variants identified by NGS were further validated using Sanger sequencing (Figure 1, Table S9).

Additionally, the variants were further annotated using the following web tools: REVEL tool [2], PolyPhen-2 [3], PMut [4], PROVEAN [5], and SIFT [6].

#### *Graphical three-dimensional models*

The SWISS-MODEL template library (<https://swissmodel.expasy.org/>, SMTL version 2019-04-24, PDB release 2019-04-19) was searched with BLAST and HHblits for evolutionary related structures matching the target sequence. Template 3e00.1.B was selected to build the homology model for PPAR $\alpha$ , which was aligned to the coordination of PPAR $\gamma$  in the PPAR $\gamma$ -RXR $\alpha$ -DNA complex structure (PDB ID: 2E00).

#### *Cell culture and transfection*

The HEK293 cells were maintained in Dulbecco's modified Eagle's medium (DMEM) (Wako, Osaka, Japan) supplemented with 10 % fetal bovine serum (FBS) (SAFC Bioscience, Brooklyn, Australia), 100 U/mL penicillin, and 100 U/mL streptomycin at 37 °C and 5 % CO<sub>2</sub>. The HEK293 cells were transfected using FuGENE HD (Promega, Madison, USA), following the manufacturer's instructions. Luciferase assay and immunocytochemistry were performed as described in the Materials and Methods section of the manuscript.

#### *In situ hybridization analysis*

Pregnant C57BL/6CrIcrIj (B6J) mice were obtained from SLC Japan (Shizuoka, Japan). At E16.5, the pregnant mice were anesthetized with pentobarbitone (100 mg/kg). The embryonic brains were fixed overnight in 30 % sucrose/4 % paraformaldehyde (PFA) in diethylpyrocarbonate (DEPC)-treated phosphate-

buffered saline (PBS). P0, P7, and adult mice were anesthetized with pentobarbitone (100 mg/kg) and transcardially perfused with 4 % PFA in PBS. The brains were excised and fixed overnight in 30 % sucrose/4 % PFA in PBS. The brains were sectioned in the coronal and sagittal planes to a thickness of 28-40  $\mu\text{m}$  using a freezing sledge microtome (Leica SM2010). The DIG-labeled probes derived from a mouse *Ppara* cDNA (FAMTOM, clone ID: C130070E08) were detected using the alkaline phosphatase-conjugated anti-DIG antibody (Roche, Basel, Switzerland) and were visualized using nitroblue tetrazolium (Nacalai, Kyoto, Japan; 350 mg/mL) and 5-bromo-4-chloro-3-indolylphosphate (Nacalai, Kyoto, Japan; 175 mg/mL). The detailed protocol has been described elsewhere [7]. The hybridization of all the sections was carried out simultaneously to compare the expression levels of each section. The images were captured using a NanoZoomer Digital Pathology (Hamamatsu Photonics, Hamamatsu, Japan).

#### *Generation of Ppara KO mice*

The first coding exon (exon 3) of the gene was targeted using the clustered regularly interspaced palindrome repeat (CRISPR)/Cas9n method in the genetic background of inbred B6J mice (Fig. S5a). The B6J zygotes obtained by *in vitro* fertilization were microinjected with the cocktail of 5 ng/mL Cas9 nickase mRNA (System Biosciences, Mountain View, CA) and 5 ng/mL each of two single guide RNAs (sgRNAs). The sgRNAs [*Ppara*-upstream (target sequence: 5'-TCCAGAGCTCTCCTCACCGATGG-3') and *Ppara*-downstream (target sequence: 5'-TTTGCAGACTACCAGTACTTAGG-3') where underlining indicates the PAM sequences] were synthesized *in vitro* using the T7 gRNA Smart Nuclease Synthesis Kit (System Biosciences), following the manufacturer's instructions. The injected zygotes were transplanted into the uterus of pseudo-pregnant dams [Crj:CD1 (ICR), Charles River Laboratories Japan]. The target region of the *Ppara* gene from the

resultant pups obtained by cesarean section was examined with direct sequencing of PCR products amplified from the template DNAs extracted from the tail. PCR was performed using the primer set A (forward 1: 5'-ATCCTGGATCTATACGTGTGTACC-3' and reverse 1: 5'-TCTGTCTCTGTGCATCTTGCTG-3' or reverse 2 (in deletion region): 5'-AGCCCGGACAGCTTCCTAAGTA-3'). The mutated alleles of the promising founders were further analyzed by sequencing the PCR products after subcloning into the pCR2.0 vector (Invitrogen). The pup that harbored a 733-bp deletion spanning exon 3 and flanking intronic regions was used as a founder (Fig. S5b). When the selected founder (#417) with a desired (loss-of-function) mutation reached sexual maturity, *in vitro* fertilization was performed with B6J strain-derived oocytes to obtain mice with heterozygous mutation allele. The successful germline transmission of the deletion to the next generation was confirmed. Heterozygotes were intercrossed to generate homozygotes (hereafter called *Ppara* KO mice) and control wild-type (WT) littermates. The total loss of Ppara protein was confirmed in the liver of the KO mouse using western blotting (Fig. S5c). Routine genotyping of mice was performed using PCR with the primer set A and agarose gel electrophoresis.

#### *Western blotting*

The livers of *Ppara* KO mice were subjected to sonication in lysis buffer [50 mM Tris-HCl (pH 8.0), 150 mM NaCl, 1 mM EDTA, 0.05 % sodium dodecyl sulfate (SDS), 0.5 % deoxycholic acid sodium salt, 1 % Triton-X100] containing protease inhibitors [1 mM phenylmethylsulfonyl fluoride (PMSF), 1.2 µg/ml aprotinin]. The cell lysates were centrifuged at 4 °C for 15 min at maximum speed. The proteins in the supernatant were subjected to SDS-polyacrylamide gel electrophoresis using a 12 % gel. The resolved proteins were transferred to a polyvinyl difluoride (PVDF)

membrane (Millipore, Bedford, MA, USA) using a transfer buffer (192 mM glycine, 100 mM Tris base, 20 % methanol). The membrane was blocked with 5 % skim milk in PBS containing 0.1 % Tween 20 (PBS-T) and 5 % skim milk for 1 h. Next, the membrane was incubated with the anti-PPAR $\alpha$  mouse monoclonal primary antibody (1:100 dilution; H-2; Santa Cruz Biotechnology, Santa Cruz, CA, USA) and GAPDH antibody (1:5000 dilution; V-18; Santa Cruz Biotechnology) prepared in blocking buffer. The membrane was washed and incubated with the horseradish peroxidase-conjugated anti-mouse antibody (1:3000 dilution; GE Healthcare Life Science Little Chalfont, UK) and anti-goat antibody (1:5000 dilution; Santa Cruz Biotechnology) prepared in blocking buffer. The bound antibodies were detected using Immobilon Western Chemiluminescent HRP Substrate (Merck, Darmstadt, Germany). The chemiluminescence was visualized using the Luminoimage analyzer Fusion SOLO S (Vilber-Lourmat, Marne-la-Vallée, France).

#### *Blood biochemistry*

Blood biochemical analyses were performed using FUJI DRI-CHEM slides and automated chemistry analyzer (FUJI DRI-CHEM 3500V, FUJIFILM, Tokyo, Japan).

#### *Behavioral analyses*

The criterion for the selection of behavioral tests: Behavioral tests were selected based on whether they were related to schizophrenia or disrupted PPAR $\alpha$  expression. Schizophrenia-related behaviors: (1) Prepulse inhibition test can measure sensorimotor gating [8]. (2) Y-maze is useful to test cognitive function, such as working memory [8]. (3) Three-chamber social interaction test can be employed to study social affiliation and social memory [9]. (4) The MK-801-induced locomotor hyperactivity test can evaluate sensitivity to psychotomimetic drugs [10]. (5) Forced swim test can evaluate the immobility behavior related to the negative symptoms of

schizophrenia [11, 12]. (6) Sucrose preference test is to evaluate an anhedonia-relevant phenotype, which is related to negative symptoms of schizophrenia [13, 14]. *Ppara* KO-related behaviors: *Ppara* KO mice showed behavioral changes as follows; (1) Burying more marbles in the marble-burying test, (2) Significant impairment in spontaneous alternation in the Y-maze test, (3) A preference for the familiar object in the novel object recognition test [15].

Decreased *Ppara* expression-related behaviors; (1) Increased immobility time in the tail suspension test, (2) Decreased locomotor activity in the open-field test, (3) Poor performance in the Y-maze test, (4) Higher sensitivity to MK-801 in the MK-801-induced locomotor hyperactivity test [16].

Forced swim test: The forced swim test was performed following a previously reported method [17]. The mice were forced to swim for 6 min in a transparent acrylic cylinder (internal diameter 20 cm, height 20 cm) that contained water to a depth of 10 cm. The first-minute data were excluded since including the data made it difficult to interpret the treatment's potential effects due to too much movement [18]. The immobility time was calculated for the remaining time period. The temperature of the water was 25°C.

Tail suspension test: An automated tail suspension apparatus with four channels were used to measure immobility during a 10-min session. The mice were suspended from a hook by the tail using non-irritating adhesive scotch tape. Immobility was detected using a charge-coupled device (CCD) camera. The duration of immobility was analyzed using Image J TS4 (O'Hara & Co., Ltd.). The first minute of the test was not used for the analysis due to too much movement. The time spent immobile during the remaining 9 min was determined.

Sucrose preference test: To test the preference for sweet taste, the mice were placed in the test cage provided with two bottles. Before the test initiation, the mice were allowed to drink tap water from the two bottles for three days. Next, the content of



one of the two bottles was changed to 1 % sucrose. The positions of the two bottles were alternated every 24 h. The liquid intake was estimated from the bottle weight. The sucrose preference was calculated as a percentage of total liquid intake and was averaged over 3 days of testing [19].

Open field test: The mice behavior was recorded in the open field (500 × 500 × 300 mm; W × D × H; gray acrylic walls, bright-light conditions at 70 lux) for 10 min. An open field monitoring system equipped with four monitoring channels was used (O'Hara & Co., Ltd.). The total distance traveled for 10 min and the percentage of time spent in the center area (size: 25 % of the field) was assessed using the automatic monitoring system Time OFCR4 (O'Hara & Co., Ltd.).

Y-maze test: Y-maze was prepared from gray acryl and comprised three arms (arm length, 40 cm; arm bottom width, 3 cm; arm upper width, 10 cm; the height of the wall, 12 cm). There were no patterns on the arm walls or external cues that facilitate the differentiation of each arm in Y-maze. The mice were placed in the center of the Y-maze field. The number of entries and alterations were recorded using a modified version of the Time YM2 program (O'Hara & Co., Ltd.). The data were collected for 7 min.

Three-chamber social interaction test: Three-chamber social interaction test was performed as described previously [20] in an apparatus with a three-chamber box (618 × 400 × 220 mm; W × D × H) and a lid equipped with a CCD camera. The test was comprised of three sessions: habituation, sociability test, and novelty test. (1) Habituation: the test mouse was put in the empty three-camber box and freely moved in the three-chamber box to habituate there. (2) Sociability test: the target mouse (B6/J) was put on one side of the three-chamber cage as target 1. The target mice and test mice were purchased from different breeders. Before the test, the target mice stayed in a different room because target mice should have different smells from the breeding room. The target mice was two weeks younger than the test mice. On the

other side of the three-chamber cage, a hexagonal object with a black and white vertical stripe (220 g) was placed. (3) Novelty test: The target mouse was in the same three-chamber cage as target 1. A new target mouse was put on the other side of the three-chamber cage as target 2. The number of approaches to the target mouse or object, and the time around the target mouse or object, the distance for ten minutes was analyzed with the software Time CS1 system (O'Hara & Co., Ltd.). Each test was carried out for ten minutes. The lighting level inside the box was 30 lux.

Novel object recognition test (NORT): The novel object recognition test was performed as described previously [21]. The apparatus for this task was an open field box (500 × 500 × 300 mm; W × D × H). The analysis of novel object recognition was performed using the Time OFCR4 system (O'Hara & Co., Ltd.). NORT takes five days. (1) First to the third day: For habituation, the mice moved freely for 15 min per day with no objects. (2) Fourth day: Transmission test was performed. Objects (pottery) were placed on the diagonals of 17 cm from the left and right inner corners of the device. The data were acquired for 10 min. (3) Fifth day: Retention test was performed. One object was changed to another object (wooden cone). The data were recorded for 10 minutes.

MK-801-induced locomotor hyperactivity test: The locomotor responses to treatment with dizocilpine maleate (MK-801) were individually evaluated in the test cage. The mouse was moved from home cages to a test cage, 1 day before the examination, and then habituated to the new environment. Recordings of locomotor were started 1 h prior to the MK-801 injection. The mice were then briefly removed from the cage and injected subcutaneously with MK-801 (0.3 mg /kg body weight) (Tocris Bioscience, Bristol, United Kingdom) dissolved in 0.9 % saline solution. The mice were immediately returned to the same test cage, and the locomotor responses to MK-801 were monitored for 3 h. The same test cage was used throughout the analysis. Locomotor activity was measured using an infrared sensor (Supermex;

Muromachi Kikai, Tokyo, Japan).

Homecage activity test: The homecage activity test was conducted to examine whether the *Ppara* KO mice show abnormal locomotor activity in a steady-state. The test was done as the preliminary experiment before the MK-801-induced locomotor hyperactivity test. The locomotor activity was individually measured in the homecage (196 × 306 × 166 cm; W × D × H) with an infrared sensor on the ceiling (Supermex; Muromachi Kikai). The heat received from the mouse per second was counted by an infrared sensor, converted into an electric signal, and further converted into a count of mouse movements. The data were accumulated at 10-minute intervals. The mice were monitored for 24 hours in a 12-hour light/dark cycle.

#### *RNA-seq analysis*

Total RNA was extracted from the mPFC using the miRNeasy Mini Kit (QIAGEN). The cDNA libraries were generated from total RNA sample [2.0 µg, RNA integrity number (RIN) ≥ 8.7] using the TruSeq Stranded mRNA Sample Prep Kit, following the manufacturer's instructions (Illumina, San Diego, CA, USA). The quality of cDNA libraries was assessed using a 2100 Bio-Analyzer (Agilent, Santa Clara, CA). The cDNA libraries were further sequenced in the 150-bp paired-end read format on the NovaSeq 6000 platform (Illumina).

The sequencing reads were mapped to the mouse genome sequence (NCBI, GRCm38/mm10) using STAR (v.2.6.0c). The expression levels were quantified using the Genedata Profiler Genome software (v.13.0.11) (Genedata, Basel, Switzerland) based on the read mapping. They were expressed as fragments per kilobase of transcript per million mapped reads (FPKM), which corresponded to the mouse's genetic information on the UCSC genome browser (<http://hgdownload.soe.ucsc.edu/goldenpath/mm10/database/refFlat.txt.gz>). The genes with FPKM < 1 or fragments < 16 in all the samples were removed before

differential expression analysis.

The differential expression among the comparison groups was statistically assessed using the Excel software (Microsoft, Redmond, WA, USA). The significant change in expression was defined based on the following criteria:  $\log_2 |\text{fold change}| > 0.1$  or  $< -0.1$  and  $p\text{-value} < 0.05$  [Student's  $t$ -test on log-transformed FPKM values ( $\log_2$  FPKM)]. Pathway enrichment was performed using IPA (QIAGEN). The heatmaps were generated using Heatmapper (<http://www.heatmapper.ca/expression/>). The statistical significance of the enriched canonical signaling pathways was calculated using Fischer's exact test. The differences were considered statistically significant when the  $p$ -value was less than 0.05.

## References

- [1] Van der Auwera GA, Carneiro MO, Hartl C, Poplin R, Del Angel G, Levy - Moonshine A, et al. From FastQ data to high - confidence variant calls: the genome analysis toolkit best practices pipeline. *Current protocols in bioinformatics* 2013;43(1):11.0. 1-.0. 33.
- [2] Ioannidis NM, Rothstein JH, Pejaver V, Middha S, McDonnell SK, Baheti S, et al. REVEL: An Ensemble Method for Predicting the Pathogenicity of Rare Missense Variants. *The American Journal of Human Genetics* 2016;99(4):877-85.
- [3] Adzhubei IA, Schmidt S, Peshkin L, Ramensky VE, Gerasimova A, Bork P, et al. A method and server for predicting damaging missense mutations. *Nat Methods* 2010;7(4):248-9.
- [4] Lopez-Ferrando V, Gazzo A, de la Cruz X, Orozco M, Gelpi JL. PMut: a web-based tool for the annotation of pathological variants on proteins, 2017 update. *Nucleic Acids Res* 2017;45(W1):W222-W8.
- [5] Choi Y, Sims GE, Murphy S, Miller JR, Chan AP. Predicting the functional

- effect of amino acid substitutions and indels. *PLoS One* 2012;7(10):e46688.
- [6] Sim NL, Kumar P, Hu J, Henikoff S, Schneider G, Ng PC. SIFT web server: predicting effects of amino acid substitutions on proteins. *Nucleic Acids Res* 2012;40(Web Server issue):W452-7.
- [7] Hauptmann G. *In situ hybridization methods*. New York: Humana Press; 2015.
- [8] Yee BK, Singer P. A conceptual and practical guide to the behavioural evaluation of animal models of the symptomatology and therapy of schizophrenia. *Cell Tissue Res* 2013;354(1):221-46.
- [9] Kaidanovich-Beilin O, Lipina T, Vukobradovic I, Roder J, Woodgett JR. Assessment of social interaction behaviors. *J Vis Exp* 2011(48).
- [10] Powell CM, Miyakawa T. Schizophrenia-relevant behavioral testing in rodent models: a uniquely human disorder? *Biol Psychiatry* 2006;59(12):1198-207.
- [11] Chatterjee M, Jaiswal M, Palit G. Comparative evaluation of forced swim test and tail suspension test as models of negative symptom of schizophrenia in rodents. *ISRN Psychiatry* 2012;2012:595141.
- [12] Chindo BA, Adzu B, Yahaya TA, Gamaniel KS. Ketamine-enhanced immobility in forced swim test: a possible animal model for the negative symptoms of schizophrenia. *Prog Neuropsychopharmacol Biol Psychiatry* 2012;38(2):310-6.
- [13] Geyer M, Markou A. Animal Models of psychiatric disorders. *Psychopharmacology (Berl)* 1995;the fourth generation of progress.:787–98.
- [14] Nestler EJ, Hyman SE. Animal models of neuropsychiatric disorders. *Nat Neurosci* 2010;13(10):1161-9.
- [15] D'Agostino G, Cristiano C, Lyons DJ, Citraro R, Russo E, Avagliano C, et al. Peroxisome proliferator-activated receptor alpha plays a crucial role in behavioral repetition and cognitive flexibility in mice. *Mol Metab*

2015;4(7):528-36.

- [16] Maekawa M, Watanabe A, Iwayama Y, Kimura T, Hamazaki K, Balan S, et al. Polyunsaturated fatty acid deficiency during neurodevelopment in mice models the prodromal state of schizophrenia through epigenetic changes in nuclear receptor genes. *Transl Psychiatry* 2017;7(9):e1229.
- [17] Yoshikawa T, Watanabe A, Ishitsuka Y, Nakaya A, Nakatani N. Identification of multiple genetic loci linked to the propensity for "behavioral despair" in mice. *Genome Res* 2002;12(3):357-66.
- [18] Can A, Dao DT, Arad M, Terrillion CE, Piantadosi SC, Gould TD. The mouse forced swim test. *J Vis Exp* 2012(59):e3638.
- [19] Aizawa F, Ogaki Y, Kyoya N, Nishinaka T, Nakamoto K, Kurihara T, et al. The Deletion of GPR40/FFAR1 Signaling Damages Maternal Care and Emotional Function in Female Mice. *Biol Pharm Bull* 2017;40(8):1255-9.
- [20] Crawley JN. Designing mouse behavioral tasks relevant to autistic-like behaviors. *Ment Retard Dev Disabil Res Rev* 2004;10(4):248-58.
- [21] Hashimoto K, Fujita Y, Shimizu E, Iyo M. Phencyclidine-induced cognitive deficits in mice are improved by subsequent subchronic administration of clozapine, but not haloperidol. *Eur J Pharmacol* 2005;519(1-2):114-7.

## Supplementary Figure Legends

### Fig. S1

Next generation sequencing based on molecular inversion probes (MIPs) for detecting variants in patients with schizophrenia.

MIPs are single-stranded oligonucleotides with a common backbone, two “targeting arms” (complementary to the target in the genome), and “molecular tags.” After probe hybridization to the genome, the subsequent sequence gap is filled by a polymerase and sealed by a ligase. Exogenous host DNA and linear probes are digested with exonucleases, which circularize the single-stranded probes. The capture region is amplified utilizing the universal primers.

### Fig. S2

Timeline of behavioral tests in *Ppara* KO mice.

### Fig. S3

Three missense variants in the PPAR $\alpha$  protein structure.

(a) Model structures of the PPAR $\alpha$  His117Gln, Arg141Cys, and Arg226Trp variants, which were generated using SWISS-MODEL and based on the crystal structure of the PPAR $\gamma$ -RXR $\alpha$  heterodimer (PDB: 3E00).

(b) Structural relationship between PPAR $\alpha$  His117 and Zinc finger 1.

(c) Structural relationship between PPAR $\alpha$  Arg141 and Zinc finger 2.

### Fig. S4

Functional analyses of PPAR $\alpha$  mutants.

(a) Relative activity of PPAR $\alpha$  mutants as a transcription factor in the HEK293 cells.

The values represent mean  $\pm$  standard deviation. The data were analyzed using one-way

analysis of variance (*ANOVA*) ( $p < 0.001$ ), followed by Dunnett's multiple comparisons test.

(b) Intracellular localization of the PPAR $\alpha$  protein was observed under a confocal microscope. Scale bar = 30  $\mu$ m

### **Fig. S5**

Distribution of *Ppara* transcripts in the brain.

*In situ* hybridization of *Ppara* on the coronal sections (a) and sagittal sections (b) of mouse brains at E16.5, P0, P7, and adult age. At E16.5, *Ppara* was highly expressed in the whole brain, especially around the lateral ventricle. At P0, the *Ppara* transcript was also detected ubiquitously in the whole brain. At P7 and adult stages, the *Ppara* transcript was weakly observed in the cortex (Cx), hippocampus (Hip), and cerebellum (Cb). The *Ppara* transcript was not detected in the corpus callosum (cc) or anterior commissure (ac). Scale bar = 1 mm

### **Fig. S6**

Generation of *Ppara* knockout (KO) mouse using the clustered regularly interspaced palindrome repeat (CRISPR)-Cas9n technology.

(a) Schematic illustration of the *Ppara* gene structure and Cas9n targeting scheme. The single guide RNA (sgRNA) targets and protospacer adjacent motifs (PAMs) are indicated in blue and magenta, respectively. Predicted Cas9n cutting sites are shown with arrowheads.

(b) PCR genotyping to detect the genomic deletion.

(c) Western blotting using the anti-PPAR $\alpha$  antibody. **The asterisk (\*) shows background signal.**

(d) Gross morphology of *Ppara* KO mice.



**Fig. S7**

(a) Average spine density in wild-type (WT) (4 mice, ten cells) and *Ppara* heterozygous mice (4 mice, 10 cells) mice. The values represent the mean  $\pm$  standard error. The data were analyzed using the unpaired *t*-test.

(b) Morphological classification of spines in WT (4 mice, ten cells) and *Ppara* heterozygous mice (4 mice, ten cells) mice. Spines were classified as immature (filopodia + thin) spines and mature (stubby + mushroom + branched) spines. The values represent the mean  $\pm$  standard error. The data were analyzed using the unpaired *t*-test.

**Fig. S8**

Heatmaps showing differentially expressed genes enriched in the sumoylation (a) and stearate biosynthetic pathways (b).

**Fig. S9**

Effects of PPAR $\alpha$  agonist on dendritic spine density.

(a) Typical images of dendritic spines in the medial prefrontal cortex (mPFC) of phencyclidine (PCP)-administered mice at 8 weeks of age. Scale bar = 1  $\mu$ m.

(b) Spine density in saline-administered (4 mice, 8 cells) and PCP-administered mice (3 mice, 7 cells). The values represent mean  $\pm$  standard error. The data were analyzed using the unpaired *t* tests.

(c) Typical images of dendritic spines in the mPFC of saline/vehicle-, saline/fenofibrate-, PCP/vehicle-, PCP/fenofibrate-administered mice at 12 weeks of age. Scale bar = 1  $\mu$ m.

(d) Spine density in saline/vehicle (6 mice, 23 cells), saline/fenofibrate- (6 mice, 11 cells), PCP/vehicle- (5 mice, 16 cells), PCP/fenofibrate- (5 mice, 16 cells) administered mice. The values represent mean  $\pm$  standard error. The data were analyzed using one-

way *ANOVA* ( $p = 0.224$ ), followed by Tukey's test.

**Table S1. Primer sequences for site-directed mutagenesis**

Primer name	PCR primer sequence
PPARA_H117Q_pcDNA3-sense	5' -GAGTCCAAGCGTGTGAAGGCTGCAAG- 3'
PPARA_H117Q_pcDNA3-antisense	5' -CACACGCTTGGACTCCGTAATGATAG- 3'
PPARA_R141C_pcDNA3-sense	5' -GTGCGACTGCAGCTGCAAGATCCAG- 3'
PPARA_R141C_pcDNA3-antisense	5' -CAGCTGCAGTCGCACTTGTCATACACC- 3'
PPARA_R226W_pcDNA3-sense	5' -CAAAGCCTGGGTCATCCTCTCAGGAAA- 3'
PPARA_R226W_pcDNA3-antisense	5' -ATGACCCAGGCTTTGACCTTGTTTCAT- 3'
PPARA_C122S_pcDNA3-sense	5' -GAAGGCAGCAAGGGCTTCTTTCGGC- 3'
PPARA_C122S_pcDNA3-antisense	5' -GCCCTTGCTGCCTTCACACGCGTGGAC- 3'
PPARA_R128T_pcDNA3-sense	5' -TTTCGGACAACGATTCGACTCAAGCT- 3'
PPARA_R128T_pcDNA3-antisense	5' -AATCGTTGTCCGAAAGAAGCCCTTGCA- 3'

**Table S2. Predicted impact of missense mutations on the protein function using Web-tools that predict the effect of amino acid changes.**

	Gene	Amino acid change	MAF <sup>a</sup> (alternation alleles /total alleles)	REVEL	PolyPhen-2	PMut	PROVEAN	SIFT
Schizophrenia	<i>RXRA</i>	p.Gln46His	0.00042 (1/2,400)	0.23	0.000	0.15	-0.253	0.14
		p.Gly60Ser	0.00042 (1/2,400)	0.47	0.327	0.17	0.290	0.34
		p.Pro63Leu	0.00083 (2/2,400)	0.30	0.015	0.27	-1.219	0.25
		p.Ser222Leu	0.00042 (1/2,400)	0.11	0.215	<b>0.52</b>	<b>-3.779</b>	0.67
		p.Thr365Met	0.00042 (1/2,400)	<b>0.89</b>	<b>0.999</b>	<b>0.72</b>	<b>-4.285</b>	<b>0.01</b>
	<i>RXRB</i>	p.Pro98Ala	0.00042 (1/2,400)	0.28	0.003	0.13	-0.519	0.17
		p.Pro104Ser	0.00042 (1/2,400)	0.34	<b>0.993</b>	0.11	0.394	0.39
		p.Pro194Leu	0.00042 (1/2,400)	0.32	<b>0.984</b>	0.41	-1.544	<b>0.02</b>
	<i>RXRG</i>	p.Pro62Leu	0.00083 (2/2,400)	<b>0.73</b>	0.896	0.45	-2.328	<b>0.01</b>
		p.Ala85Val	0.00042 (1/2,400)	0.26	0.183	0.12	-0.517	<b>0.03</b>
		p.Arg195His	0.00042 (1/2,400)	<b>0.97</b>	<b>1.000</b>	<b>0.91</b>	<b>-4.259</b>	<b>0.00</b>
	<i>PPARA</i>	p.His117Gln	0.00042 (1/2,400)	<b>0.70</b>	<b>1.000</b>	<b>0.74</b>	<b>-5.889</b>	<b>0.03</b>
		p.Asp140Asn	0.00460 (11/2,400)	0.41	0.647	0.20	-1.184	0.87
		p.Arg141Cys	0.00042 (1/2,400)	<b>0.83</b>	<b>1.000</b>	<b>0.73</b>	<b>-3.484</b>	<b>0.01</b>

		p.Arg226Trp	0.00042 (1/2,400)	<b>0.80</b>	<b>1.000</b>	<b>0.68</b>	<b>-5.799</b>	<b>0.01</b>
		p.Val227Ala	0.05309 (121/2,400)	0.08	0.000	0.06	1.080	1.00
		p.Gly395Glu	0.00629 (15/2,400)	0.22	0.052	0.23	1.856	1.00
	<i>PPARD</i>	p.Asn30Ser	0.00042 (1/2,400)	0.16	0.000	0.12	-0.376	0.27
		p.Thr208Met	0.00042 (1/2,400)	0.15	<b>0.982</b>	0.24	-1.790	0.15
		p.Glu382Lys	0.00042 (1/2,400)	<b>0.56</b>	0.915	0.26	-1.046	0.70
	<i>PPARG</i>	p.Pro12Ala	0.03270 (76/2,400)	0.24	0.000	0.10	-0.047	<b>0.00</b>
		p.Lys184Glu	0.00042 (1/2,400)	<b>0.97</b>	<b>0.998</b>	<b>0.93</b>	<b>-2.933</b>	<b>0.01</b>
		p.Glu371Lys	0.00042 (1/2,400)	0.42	0.130	0.26	0.025	0.38
ToMMo	<i>RXRA</i>	p.Pro8Leu	0.00014 (1/6,916)	0.34	0.581	0.21	-0.713	1.00
3.5KJPN		p.Thr23Met	0.00014 (1/6,898)	0.33	0.617	0.22	-0.556	<b>0.02</b>
		p.Gln46His	0.00029 (2/6,900)	0.23	0.000	0.14	-0.253	0.14
		p.Gly60Ser	0.00073 (5/68,92)	0.47	0.327	0.17	0.290	0.34
		p.Thr81Ile	0.00015 (1/6,520)	0.34	0.004	0.33	-1.400	<b>0.02</b>
		p.Gly212Val	0.00015 (1/6,892)	0.12	0.027	0.41	-1.355	0.38
		p.Lys213Asn	0.00015 (1/6,886)	0.22	0.911	<b>0.58</b>	<b>-3.429</b>	0.33

	p.Val242Met	0.00014 (1/6,978)	0.27	0.916	<b>0.53</b>	-2.272	<b>0.02</b>
	p.Thr365Met	0.00014 (1/7,022)	<b>0.89</b>	<b>0.999</b>	<b>0.72</b>	<b>-4.285</b>	<b>0.01</b>
<i>RXRB</i>	p.Pro182Ser	0.00030 (2/6,696)	<b>0.52</b>	<b>1.000</b>	0.47	<b>-2.689</b>	<b>0.02</b>
	p.Ala295Val	0.00014 (1/6,938)	0.14	0.019	0.24	-1.127	0.37
	p.Arg303Gly	0.00014 (1/6,944)	<b>0.51</b>	0.526	0.42	<b>-4.730</b>	0.10
	p.Arg468Gln	0.00015 (1/6,860)	<b>0.86</b>	<b>1.000</b>	Invalid	<b>-3.501</b>	0.43
<i>RXRG</i>	p.Thr25Ile	0.00014 (1/7,078)	0.40	<b>0.997</b>	0.25	-0.706	0.10
	p.Pro38Ser	0.00014 (1/7,084)	0.21	0.000	0.25	-0.292	0.72
	p.Ala85Val	0.00084 (6/7,102)	0.26	0.183	0.12	-0.517	<b>0.03</b>
	p.Pro95Thr	0.00028 (2/7,094)	0.28	0.183	0.08	-0.393	0.42
	p.Gly132Glu	0.00014 (1/7,106)	0.37	0.898	0.35	-1.363	1.00
	p.Gly152Arg	0.00014 (1/7,108)	<b>0.96</b>	<b>1.000</b>	<b>0.87</b>	<b>-6.302</b>	<b>0.00</b>
	p.Arg335Gln	0.00028 (2/7,090)	<b>0.91</b>	<b>1.000</b>	<b>0.79</b>	<b>-3.686</b>	0.06
	p.Asn386Ser	0.00014 (1/7,088)	0.13	0.011	0.44	-0.377	0.36
	p.Arg427His	0.00014 (1/7,048)	<b>0.93</b>	<b>1.000</b>	<b>0.79</b>	<b>-4.299</b>	<b>0.00</b>
	p.Pro447Arg	0.00014 (1/6,986)	<b>0.76</b>	<b>1.000</b>	<b>0.68</b>	<b>-7.286</b>	<b>0.03</b>
<i>PPARA</i>	p.Pro10Leu	0.00014 (1/6,968)	0.44	0.042	0.33	-1.128	0.90

	p.Pro22Arg	0.00044 (3/6,824)	<b>0.74</b>	<b>0.999</b>	<b>0.76</b>	-1.524	<b>0.00</b>
	p.Ser38Leu	0.00015 (1/6,832)	0.47	0.944	<b>0.57</b>	-1.414	<b>0.02</b>
	p.Gln39Arg	0.00015 (1/6,844)	0.23	0.000	0.26	-0.633	0.69
	p.Asp140Asn	0.00501 (35/6,988)	0.41	0.647	0.20	-1.184	0.87
	p.Leu162Val	0.00014 (1/7,032)	<b>0.67</b>	0.169	0.29	-1.761	0.06
	p.Ala170Thr	0.00014 (1/7,054)	<b>0.92</b>	<b>0.999</b>	<b>0.65</b>	<b>-3.543</b>	<b>0.00</b>
	p.Val227Ala	0.05570 (395/7,092)	0.08	0.000	0.06	1.080	1.00
	p.Arg341Cys	0.00014 (1/7,096)	<b>0.83</b>	<b>1.000</b>	<b>0.85</b>	<b>-6.336</b>	<b>0.00</b>
	p.Gly395Glu	0.00619 (44/7,106)	0.22	0.052	0.23	1.856	1.00
<i>PPARD</i>	p.Asn30Ser	0.00088 (6/6,812)	0.16	0.000	0.12	-0.376	0.27
	p.Thr208Met	0.00028 (2/7,064)	0.15	<b>0.982</b>	0.24	-1.790	0.15
	p.Arg314His	0.00014 (1/7,056)	<b>0.63</b>	0.512	0.33	<b>-3.418</b>	<b>0.01</b>
	p.Arg419Gln	0.00015 (1/6,782)	0.08	0.928	<b>0.58</b>	0.041	0.27
<i>PPARG</i>	p.Pro12Ala	0.03054 (217/7,106)	0.24	0.000	0.10	-0.047	<b>0.00</b>
	p.Asp15Tyr	0.00042 (3/7,106)	0.16	0.301	0.14	-0.123	0.07
	p.Thr67Ala	0.00014 (1/7,104)	0.30	<b>0.999</b>	0.15	-0.777	0.30
	p.Asp69Asn	0.00014 (1/7,108)	0.26	<b>1.000</b>	0.17	-0.780	0.30

p.Tyr95Cys	0.00028 (2/7,106)	0.29	<b>0.988</b>	0.36	-0.984	<b>0.00</b>
p.Glu101Lys	0.00014 (1/7,104)	0.13	0.768	0.18	-0.989	0.12
p.Ser226Ala	0.00014 (1/7,080)	0.32	0.007	0.19	-0.320	0.34
p.Asp248Gly	0.00014 (1/7,100)	0.44	0.817	<b>0.67</b>	-2.421	0.08
p.Val276Ile	0.00014 (1/7,100)	0.19	0.497	0.26	-0.450	<b>0.05</b>
p.Arg316His	0.00014 (1/7,098)	0.43	<b>0.999</b>	0.32	-1.869	0.30
p.Ser383Gly	0.00014 (1/7,090)	<b>0.76</b>	0.160	<b>0.65</b>	<b>-3.052</b>	0.11
p.Ile414Met	0.00014 (1/7,096)	0.39	<b>0.983</b>	0.42	-0.092	<b>0.01</b>

<sup>a</sup> Minor allele frequency

<sup>b</sup> ToMMo 3.5KJPN: <https://ijgvd.megabank.tohoku.ac.jp/>

Bold characters mean that the scores exceeded the cut-off values: REVEL > 0.5, PolyPhen-2 > 0.975, PMut > 0.5, PROVEAN < -2.5 and SIFT < 0.05.

REVEL: <https://sites.google.com/site/revelgenomics/>

PhlyPhen-2: <http://genetics.bwh.harvard.edu/pph2/>

SIFT: [https://sift.bii.a-star.edu.sg/www/SIFT\\_seq\\_submit2.html](https://sift.bii.a-star.edu.sg/www/SIFT_seq_submit2.html)

PMut: <http://mmb.irbbarcelona.org/PMut/>

PROVEAN: [http://provean.jcvi.org/seq\\_submit.php](http://provean.jcvi.org/seq_submit.php)



**Table S3. Allele frequencies of four common variants in schizophrenia and ToMMo 3.5KJPN.**

Gene	Amino acid change		<i>n</i>	Allele frequency		<i>p</i> -value ( $\chi^2$ test)
<i>PPARA</i>	p.Asp140Asn	Schizophrenia	2400	A	G	0.7969
		ToMMo 3.5KJPN <sup>a</sup>	6988	11	2389	
	p.Val227Ala	Schizophrenia	2400	C	T	0.3241
		ToMMo 3.5KJPN	7092	121	2279	
	p.Gly395Glu	Schizophrenia	2400	A	G	0.9750
		ToMMo 3.5KJPN	7106	395	6697	
<i>PPARG</i>	p.Pro12Ala	Schizophrenia	2400	G	C	0.7820
		ToMMo 3.5KJPN	7106	76	2324	

<sup>a</sup>ToMMo 3.5KJPN: <https://ijgvd.megabank.tohoku.ac.jp/>

**Table S4. Association of *PPARA* Arg226Trp variant with schizophrenia.**

Gene	Amino acid change	<i>n</i>	Allele frequency		<i>p</i> -value (Fisher's exact test)
<i>PPARA</i>	p.Arg226Trp		T	C	
	Schizophrenia	2400	1	2399	
	gnomAD v2.1.1 (Exomes) <sup>a</sup>	251392	1	251391	<b>0.0188</b>

<sup>a</sup> gnomAD: <https://gnomad.broadinstitute.org/>

Bold character means significant difference ( $p < 0.05$ ).

**Table S5. Blood biochemical data of *Ppara* KO mouse (4 weeks old, female)**

	WT ( <i>n</i> = 5)	KO ( <i>n</i> = 5)	<i>p</i> -value
Aspartate aminotransferase (AST) (U/l)	94.4 ± 13.2	84.0 ± 6.4	0.50 <sup>a</sup>
Alanine aminotransferase (ALT) (U/l)	22.0 ± 1.3	35.8 ± 4.0	0.0079 <sup>b</sup>
Lactate dehydrogenase (LDH) (U/l)	328 ± 13	345 ± 26	0.58 <sup>a</sup>
Cholinesterase (CHE) (U/l)	18.8 ± 1.0	21.8 ± 1.1	0.071 <sup>a</sup>
Glucose (Glu) (mg/dl)	156 ± 21	122 ± 9	0.18 <sup>a</sup>
Total cholesterol (T-Cho) (mg/dl)	68.0 ± 9.1	59.8 ± 3.3	0.42 <sup>a</sup>
HDL cholesterol (HDL) (mg/dl)	60.6 ± 6.8	56.6 ± 4.5	0.64 <sup>a</sup>
Triglyceride (TG) (mg/dl)	98.0 ± 24.7	72.4 ± 27.1	0.51 <sup>a</sup>

Demographic variables are listed as mean ± SE.

<sup>a</sup> Unpaired *t* test

<sup>b</sup> Mann-Whitney *U*-test

All measurements were within standards reported in <https://www.criver.com>.

**Table S6. Summary of behavioral characterization of *Ppara* KO mouse**

Behavioral test		WT	KO	<i>p</i> -value
Forced-swim test	Immobility time (min)	163 ± 9 ( <i>n</i> = 11)	175 ± 8 ( <i>n</i> = 15)	0.32 <sup>a</sup>
Tail-suspension test	Immobility time (%)	59.0 ± 4.5 ( <i>n</i> = 11)	46.3 ± 4.2 ( <i>n</i> = 15)	0.035 <sup>a</sup>
Administration of MK801	Total locomotor activity /3hour (x10 <sup>4</sup> , post injection)	4.64 ± 0.34 ( <i>n</i> = 11)	5.04 ± 0.26 ( <i>n</i> = 13)	0.36 <sup>a</sup>
Sucrose preference test	Sucrose preference (%)	80.1 ± 3.8 ( <i>n</i> = 11)	82.6 ± 3.2 ( <i>n</i> = 15)	0.62 <sup>a</sup>
Open field test	Total distance (cm /15 min) (x10 <sup>3</sup> )	5.65 ± 0.46 ( <i>n</i> = 11)	5.44 ± 0.30 ( <i>n</i> = 13)	0.69 <sup>a</sup>
	Center region (%)	7.43 ± 0.99 ( <i>n</i> = 11)	6.42 ± 0.68 ( <i>n</i> = 13)	0.40 <sup>a</sup>
Y-maze test	Alternation rate (%)	61.3 ± 3.9 ( <i>n</i> = 11)	68.6 ± 2.5 ( <i>n</i> = 15)	0.12 <sup>a</sup>
	Total entry number	21.1 ± 0.8 ( <i>n</i> = 11)	21.9 ± 0.8 ( <i>n</i> = 15)	0.51 <sup>a</sup>
Three-chamber social interaction test	Sociability (%)	63.6 ± 4.5 ( <i>n</i> = 11)	73.8 ± 2.9 ( <i>n</i> = 15)	0.064 <sup>a</sup>
	Novelty (%)	75.5 ± 4.0 ( <i>n</i> = 11)	72.9 ± 1.6 ( <i>n</i> = 15)	0.54 <sup>b</sup>
Novel object recognition test	Moving speed (cm /sec)	9.43 ± 0.32 ( <i>n</i> = 11)	9.26 ± 0.23 ( <i>n</i> = 15)	0.66 <sup>a</sup>
	Training (%)	57.7 ± 1.9 ( <i>n</i> = 11)	58.0 ± 2.2 ( <i>n</i> = 15)	0.61 <sup>b</sup>
	Retention (%)	59.6 ± 6.9 ( <i>n</i> = 11)	61.3 ± 3.8 ( <i>n</i> = 15)	0.82 <sup>a</sup>

Home cage activity test	Locomotor activity (24-hour) ( $\times 10^4$ )	$7.64 \pm 0.76$ ( $n = 11$ )	$8.34 \pm 0.56$ ( $n = 15$ )	0.22 <sup>a</sup>
	Locomotor activity (dark 12-hour) ( $\times 10^4$ )	$6.89 \pm 0.71$ ( $n = 11$ )	$7.38 \pm 0.51$ ( $n = 15$ )	0.34 <sup>a</sup>

Values are mean  $\pm$  SE.

<sup>a</sup>Unpaired  $t$  test

<sup>b</sup>Mann-Whitney  $U$ -test

**Table S7. PPRE in the promoter region of synaptogenesis signaling pathway-related genes**

Symbol	Accession number	Sequence mismatches							
		0		1		2		3	
		DR1 <sup>a</sup>	DR2 <sup>b</sup>	DR1	DR2	DR1	DR2	DR1	DR2
<i>Braf</i>	NM_139294								
<i>Cdh19</i>	NM_001081386								
	NM_001356415								
<i>Creb1</i>	NM_133828								
	NM_009952								
	NM_001037726								
<i>Gria2</i>	NM_001083806								
	NM_013540								
	NM_001039195								
	NM_001357924								
	NM_001357927								
<i>Lrrtm2</i>	NM_178005								
<i>Pik3c2a</i>	NM_011083								
<i>Rps6kb1</i>	NM_001114334								
	NM_028259								
	NM_001363162								
<i>Syt14</i>	NM_001301370								
	NM_181546								
<i>Yes1</i>	NM_001205133								
	NM_001205132								
	NM_009535								
<i>Ap2a1</i>	NM_007458								
	NM_001077264								

<i>Cdh22</i>	NM_174988								
<i>Cntnap1</i>	NM_016782								
<i>Dlg4</i>	NM_007864								
	NM_0011109752								
	NM_001370671								
	NM_001370672								
	NM_001370674								
	NM_001370675								
<i>Epha10</i>	NM_001256432								
	NM_177671								
<i>Ephb6</i>	NM_001146351								
	NM_007680								
<i>Lrp1</i>	NM_08512								
<i>Nlgn2</i>	NM_198862								
	NM_001364137								
<i>Nrxn2</i>	NM_001205234								
	NM_020253								
	NM_001205235								
	NM_001369363								
<i>Pik3r2</i>	NM_008841								
<i>Prkar1b</i>	NM_008923								
	NM_001253890								
	NM_001359097								
	NM_001359099								
	NM_001359098								
	NM_001359100								
	NM_001359101								

<i>Sgta</i>	NM_001358549								
	NM_024499								
	NM_001358550								
<i>Stx1a</i>	NM_016801								
	NM_001359179								
<i>Syngap1</i>	NM_001281491								
	NM_001371033								
	NM_001371034								
<i>Syt3</i>	NM_001114116								
	NM_016663								

<sup>a</sup> DR1: direct repeat 1

<sup>b</sup> DR2: direct repeat 2

PPRE Search: <http://www.classicus.com/PPRE/>, Binding efficiency > 80, Flanking Match > 1

Boxes highlighted in yellow show the presence of the PPRE motifs in the promoter region (2000-bp upstream of TSS (transcriptional start site) of each gene).



**Table S8. Blood biochemical data after fenofibrate administration for a month  
(9 weeks old, male)**

	Control ( <i>n</i> = 8)	Fenofibrate ( <i>n</i> = 8)	<i>p</i> -value
Aspartate aminotransferase (AST) (U/l)	41.0 ± 3.8	45.9 ± 4.1	0.40 <sup>a</sup>
Alanine aminotransferase (ALT) (U/l)	20.6 ± 1.2	38.6 ± 5.8	<0.001 <sup>b</sup>
Lactate dehydrogenase (LDH) (U/l)	209 ± 10	271 ± 42	0.19 <sup>b</sup>
Creatine phosphokinase (CPK) (U/l)	157 ± 25	188 ± 47	0.58 <sup>a</sup>
Amylase (AMYL) (U/l) (x10 <sup>3</sup> )	2.35 ± 0.12	1.99 ± 0.04	0.028 <sup>b</sup>
Blood urea nitrogen (BUN) (mg/dl)	23.3 ± 1.3	26.2 ± 0.8	0.068 <sup>a</sup>
Creatinine (CRE) (mg/dl)	0.233 ± 0.063	0.156 ± 0.022	0.70 <sup>b</sup>

Demographic variables are listed as mean ± SE.

<sup>a</sup> Unpaired *t* test

<sup>b</sup> Mann-Whitney *U*-test

All measurements were within standards reported in <https://www.criver.c>

**Table S9. Primer sequences and PCR conditions used for re-sequencing of the *RXR/PPAR* genes**

Gene	Region	Primer name	PCR primer sequence	Product length (bp)	annealing (°C)
<i>RXRA</i> NM_002957	Exon 2	RXRA_E02-1F	5'- CAGGCGCAGAACAGTACCTTG -3'	687	61.5
		RXRA_E02-1R	5'- CTCGGCTGATGATCCAAAGG -3'		
	Exon 3	RXRA_E03-1F	5'- CCTTGCTGAGCAAGCACAGTG -3'	548	63.0
		RXRA_E03-1R	5'- CCAACACTCACTGTCCCACAGAC -3'		
	Exon 4	RXRA_E04-1F	5'- AGGAGCAGAGAGAGTGAGGCTG -3'	459	61.0
		RXRA_E04-1R	5'- CAGGCCACTCACTCCCTGTT -3'		
	Exon 5	RXRA_E05-1F	5'- TTGGAATTAATGAGAGTTGGCCTC -3'	547	61.5
		RXRA_E05-1R	5'- ACGGGGTCACCTCAGGTAAGA -3'		
	Exon 6	RXRA_E06-1F	5'- ATCAGGCCACACCTAATCACCT -3'	403	60.5
		RXRA_E06-1R	5'- GTGTCCTGGTACGTGTCCCAT -3'		
	Exon 7	RXRA_E07-1F	5'- TGTGCCGGTGTGTACTGTAGAAC -3'	542	60.5
		RXRA_E07-1R	5'- CAAGTGCTCCCTGTGGTTACAG -3'		
	Exon 8	RXRA_E08-1F	5'- TGTCTGGGAGTCCTTGCCTTG -3'	416	63.5
		RXRA_E08-1R	5'- AGGTGAGCAGAAGGCAGCATG -3'		
	Exon 9	RXRA_E09-1F	5'- CAAATAGTTGACCCAAGGTCACG -3'	592	61.5
		RXRA_E09-1R	5'- ATCCTTCCAGTGGGGATACGA -3'		

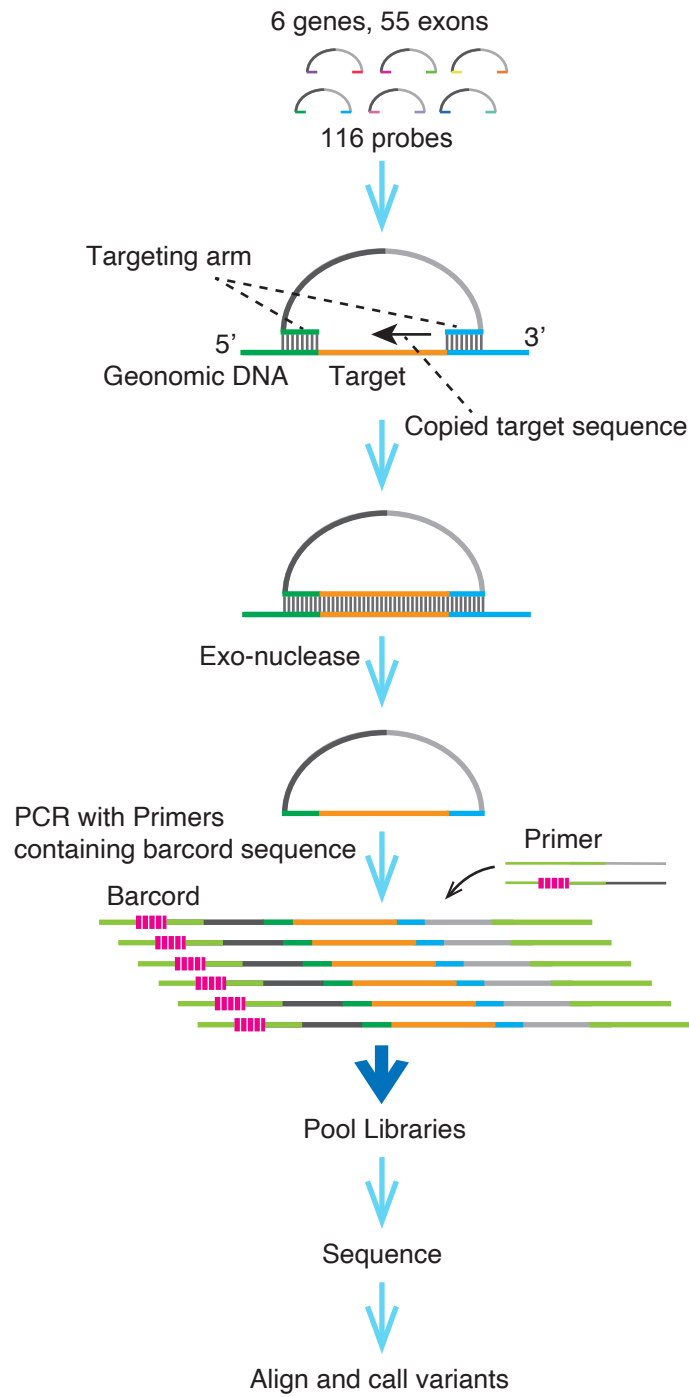
	Exon 10	RXRA_E10-1F	5'- TTGCCACTGCCTCTGTTTCCT -3'	565	63.0
		RXRA_E10-1R	5'- AGGCTGCTGCCTCAGGAAAG -3'		
<i>RXRB</i>	Exon 1 (variant 3)	RXRBv3_E01-1F	5'- CTCATTAGGTGAGGAAAAGGCCT -3'	474	60.5
NM_001291989		RXRBv3_E01-1R	5'- AAGGATTGATCGGAGGATTAGCT -3'		
<i>RXRB</i>	Exon 1	RXRB_E01-1F	5'- TCTGTACAAAGATGGCTGCCA -3'	627	60.5
NM_001270401		RXRB_E01-1R	5'- TCAAGCGGTCACAGCTAGGA -3'		
	Exon 2	RXRB_E02-1F	5'- CTGTTGTTTGACAGCAGGGTG -3'	602	60.0
		RXRB_E02-1R	5'- TGCACTGAAAGATCAGTCACCTC -3'		
	Exon 3	RXRB_E03-1F	5'- TGTTTATTCACTTTGGGGTTGTG -3'	521	59.5
		RXRB_E03-1R	5'- CTCCTTTTCCCTCTGACCTTC -3'		
	Exon 4	RXRB_E04-1F	5'- GAAGGTCAGAGGGAAAAGGAAG -3'	568	59.5
		RXRB_E04-1R	5'- AGAAGGAAACTCAAGGGCCA -3'		
	Exon 5	RXRB_E05-1F	5'- TGCCCTTTTATAACCCTTCCTTC -3'	533	60.5
		RXRB_E05-1R	5'- CAGAAGGAGCTATCACATCCACC -3'		
	Exon 6	RXRB_E06-1F	5'- GGTGGATGTGATAGCTCCTTCTG -3'	543	60.5
		RXRB_E06-1R	5'- ATCAGGCCAAGGGATTCAAA -3'		
	Exon 7, 8	RXRB_E07-1F	5'- TTGGATCCCTTTGACTTCTTGAC -3'	749	60.5
		RXRB_E08-1R	5'- ACTTGCTTGCCCTTACCAGAG -3'		
	Exon 9, 10	RXRB_E09-1F	5'- CTCAACCTGGAAATCTCCCAACT -3'	756	61.5

<i>RXRG</i> NM_006917	Exon 2	RXRB_E10-1R	5'- CTTCCAACCTTGGGATATCAAGCA -3'	639	61.5	
		RXRG_E02-1F	5'- CCTCGCTTGTCTTTATAACCACCA -3'			
	Exon 3	RXRG_E02-1R	5'- CTGGACCATGAGGAGTTGTCAGT -3'			
		RXRG_E03-1F	5'- TTCCTCCTATGGCACTTTTATCC -3'			562
	Exon 4	RXRG_E03-1R	5'- AGGGTTTCTGAAATGTTTCCTGT -3'			
		RXRG_E04-1F	5'- AATGCAGAGGAAAGACACGAGG -3'			590
RXRG_E04-1R	5'- TGCAATACACGAGTACCCAAAGTC -3'					
Exon 5, 6	RXRG_E05-1F	5'- TGCACTAAAGAACCCCTCATTCTC -3'	823	61.5		
	RXRG_E06-1R	5'- AAGCCGTGGTAAAATTTGCATG -3'				
<i>PPARA</i> NM_001001928	Exon 3	PPARA_E03-1Fb	5'- TCTTTCCTCCCAGTAGCTTGGAG -3'	551	61.5	
		PPARA_E03-1Rb	5'- AGACCATCCTGGCTAACACAGTG -3'			
	Exon 4	PPARA_E04-1F	5'- GTCAGCTCAGCAGCAGTGAGAG -3'	634	61.5	
		PPARA_E04-1R	5'- GAGACAGGGTTTCATCATGTTGG -3'			
	Exon 5	PPARA_E05-1F	5'- CGAACTCCTGACCTCAGGTGAT -3'	480	60.0	
		PPARA_E05-1Rb	5'- TCTGATTACAAAATGACTTGGGTG -3'			
	Exon 6	PPARA_E06-1F	5'- TAACGATGGTGTCCACCTTCAGC -3'	632	61.0	
		PPARA_E06-1R	5'- GTGGCTCCAAGCAAGAAGAAAG -3'			
	Exon 8	PPARA_E08-1F	5'- AGAGTACTGGTCCTGTCTGTCCCT -3'	663	60.5	
		PPARA_E08-1R	5'- CTACCCCCAGCATTTGAGTTCT -3'			

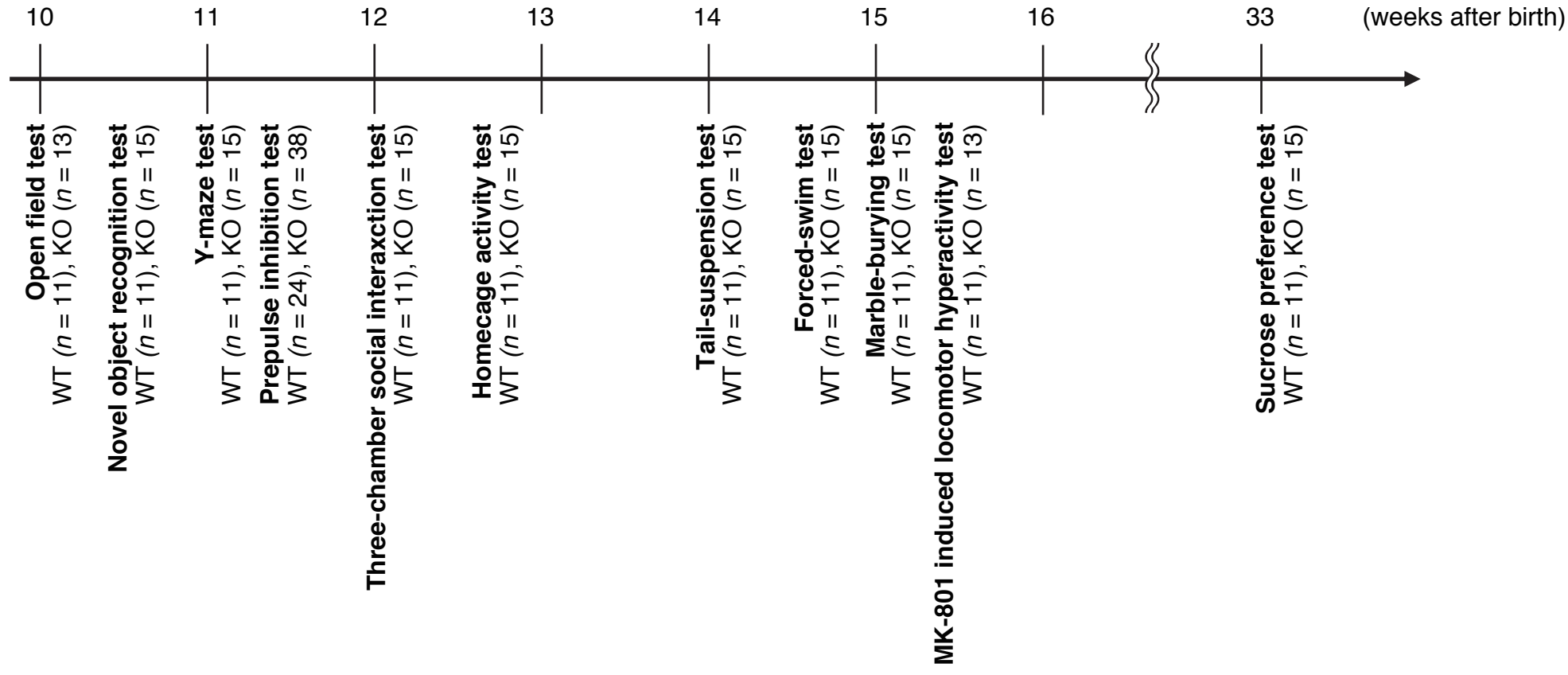
<i>PPARD</i> NM_001171818	Exon 4	PPARD_E04-1F	5'- AAACCCACTACAAGAGCCAGGT -3'	662	60.0
		PPARD_E04-1R	5'- TACAGAAGGAAGTGGTGCAGCT -3'		
	Exon 5	PPARD_E05-1F	5'- TAGGCTCTGGGAGAAATGCTG -3'	579	60.5
		PPARD_E05-1R	5'- GGTAGGCTTGACAAGGGAACC -3'		
	Exon 6	PPARD_E06-1F	5'- GAGCCACTGTGCCTGAACTAAAA -3'	553	61.5
		PPARD_E06-1R	5'- CATGGTAGATGCTGGCAGTCTG -3'		
	Exon 7	PPARD_E07-1F	5'- ATCTTGTGGAGCTTGCGATCT -3'	590	60.0
		PPARD_E07-1R	5'- ATGTCTCGATGTCGTGGATCA -3'		
	Exon 8	PPARD_E08-1F	5'- ACTTCAACATGACCAAAAAGAAGG -3'	896	59.5
		PPARD_E08-1R	5'- TTCCTGTCTCCACCTCTATCTACG -3'		
	Exon 9	PPARD_E09-1F	5'- AAGAAGTGGATTAAGACCAGGGGT -3'	633	61.5
		PPARD_E09-1R	5'- CAGGAAGAGAGCTGGCTGGA -3'		
<i>PPARG</i> NM_015869	Exon 1	PPARG_E01-1F	5'- TGCCAAAGCAGTGAACATTATGA -3'	495	61.5
		PPARG_E01-1R	5'- AAATGAACGCGATAGCAACGA -3'		
	Exon 2	PPARG_E02-1F	5'- TGGGTAAAGGGTGACTTCCTTTC -3'	604	61.5
		PPARG_E02-1R	5'- TCCCTTCCTGGCATTTCATAGA -3'		
	Exon 4	PPARG_E04-1F	5'- AAGGGACCTGGAGATCCTCTG -3'	574	60.5
		PPARG_E04-1R	5'- GTCTCTTTTCTCCTCATGGCAGA -3'		
	Exon 6	PPARG_E06-1F	5'- TGGTGAAATATGTTTGGTCCCA -3'	840	60.5

PPARG\_E06-1R 5'-CTTCACACCGCAAACCTATGAC-3'

---

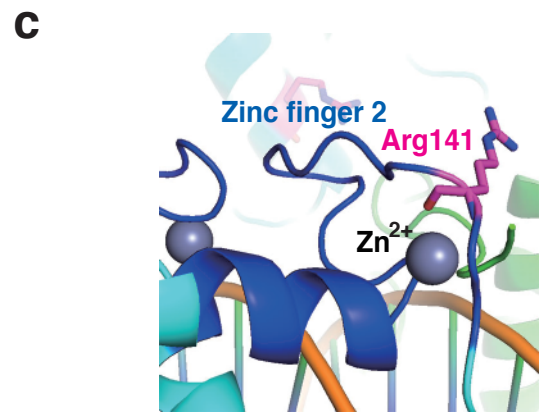
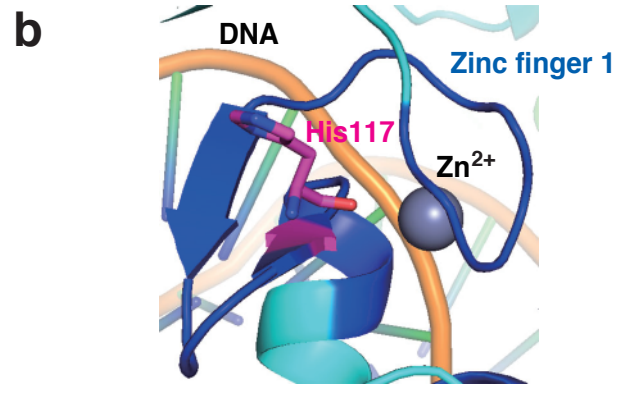
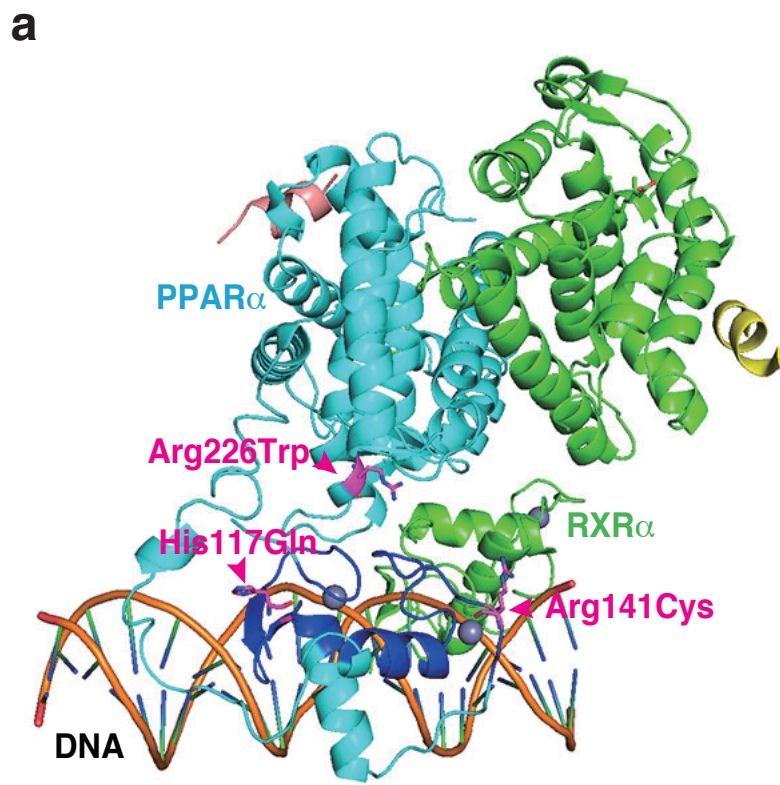


**Figure S1**

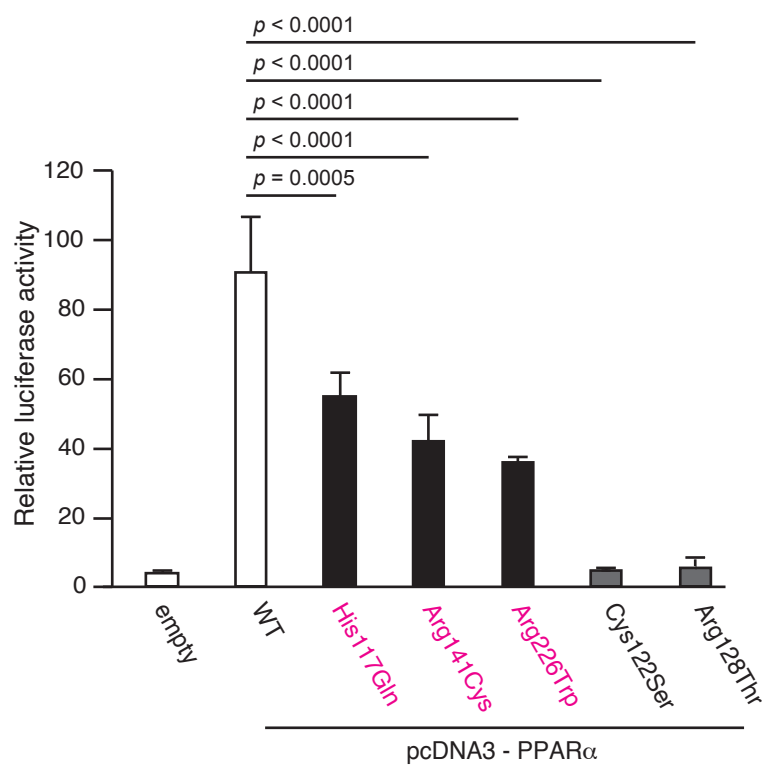
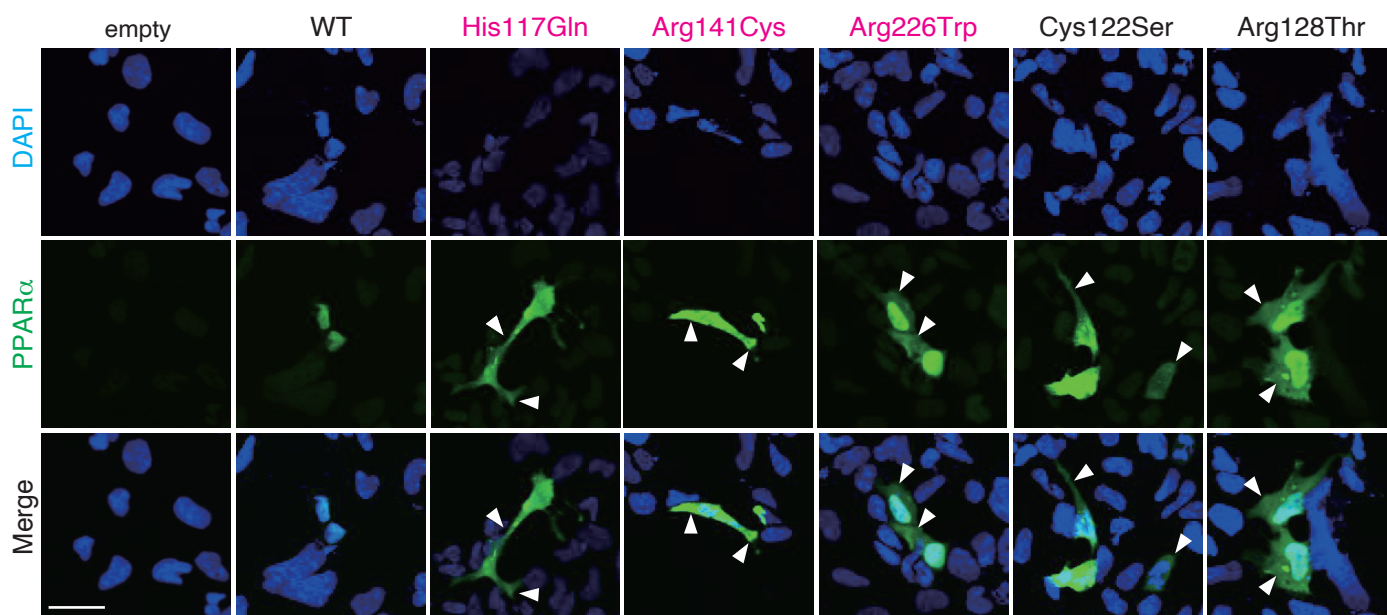


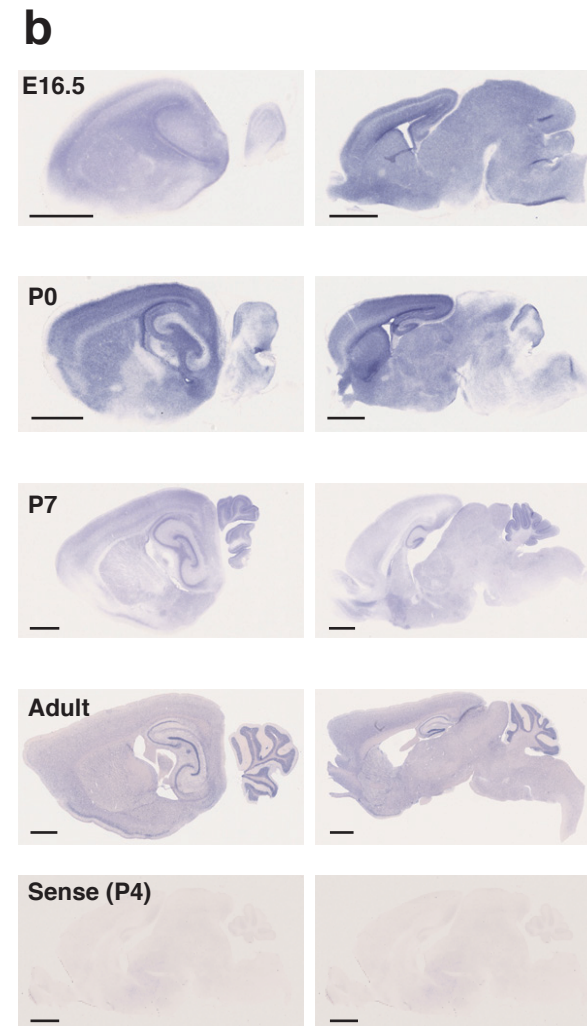
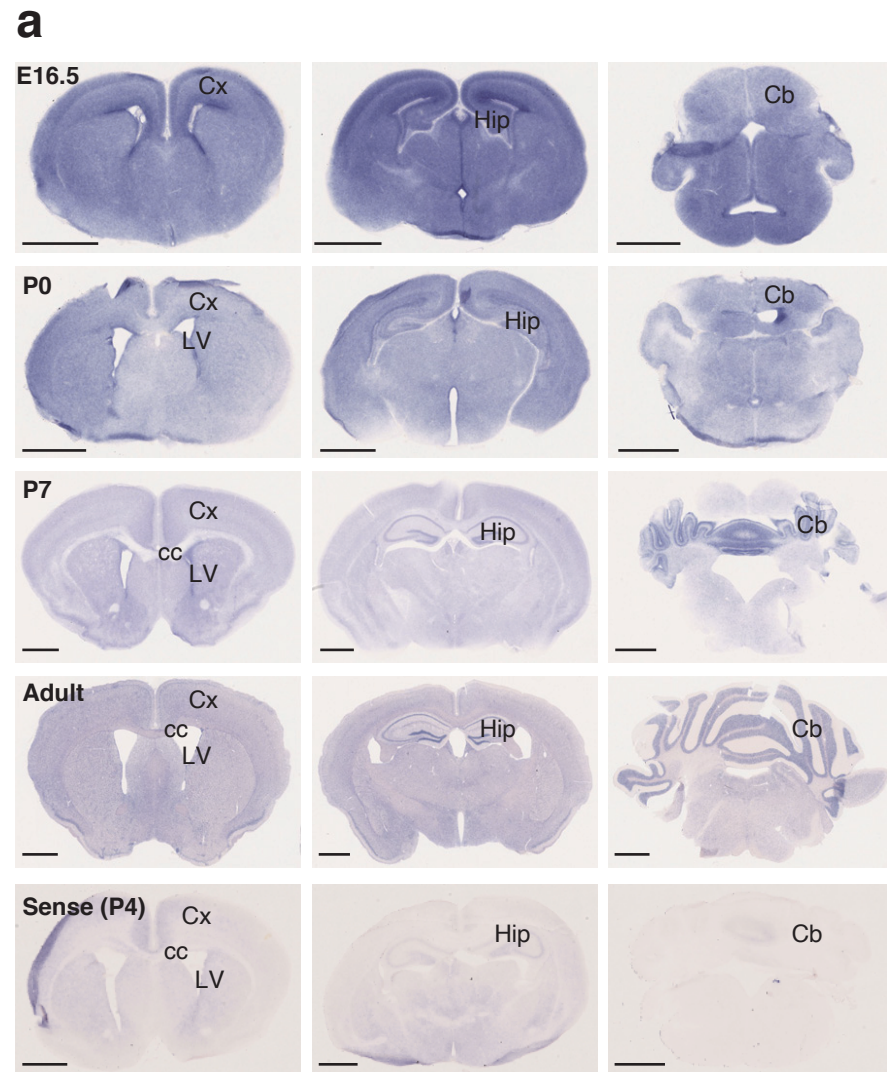
**Figure S2**



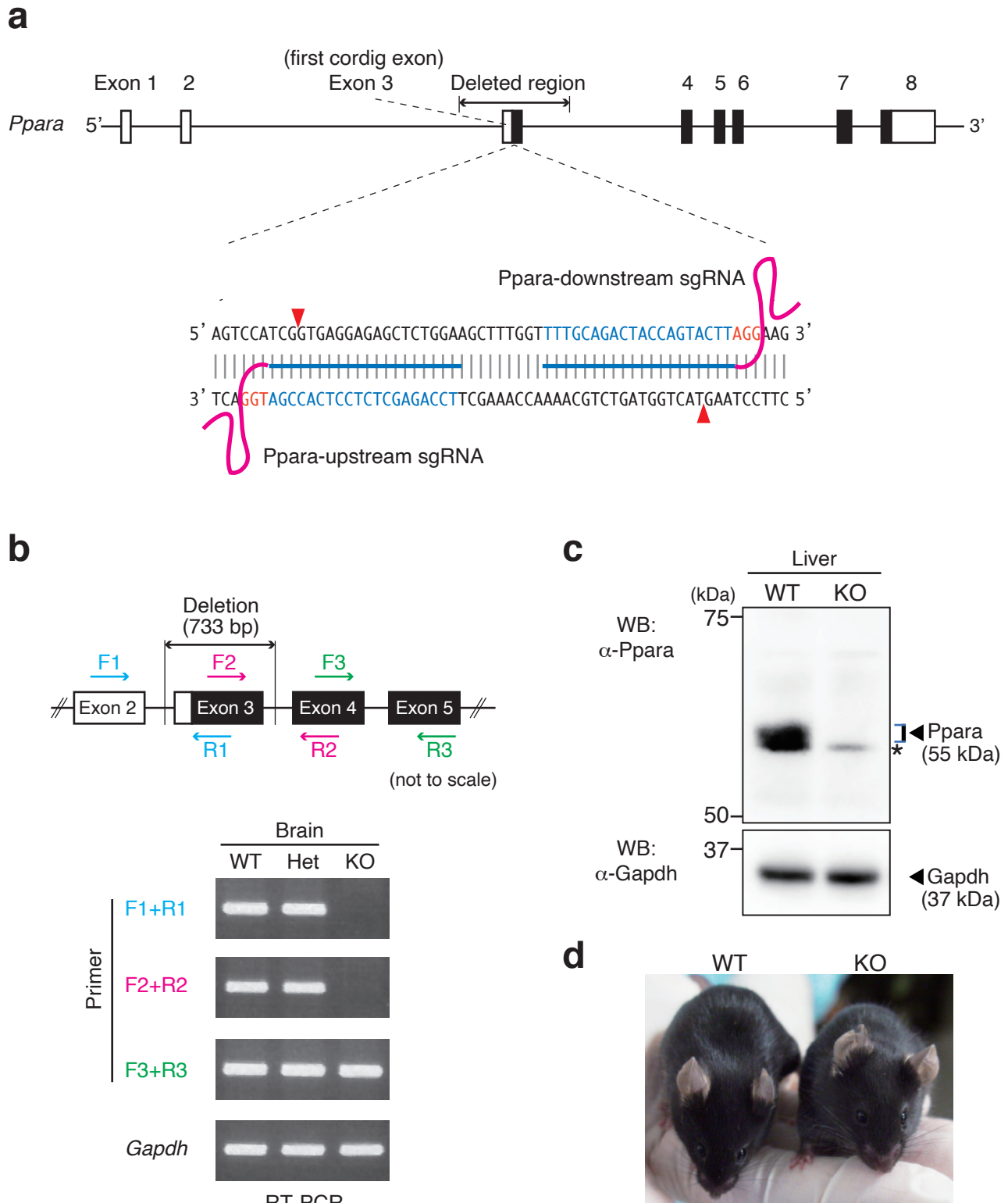


**Figure S3**

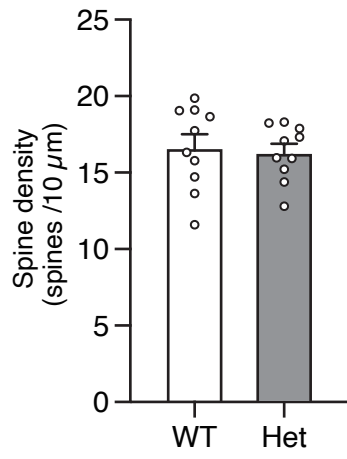
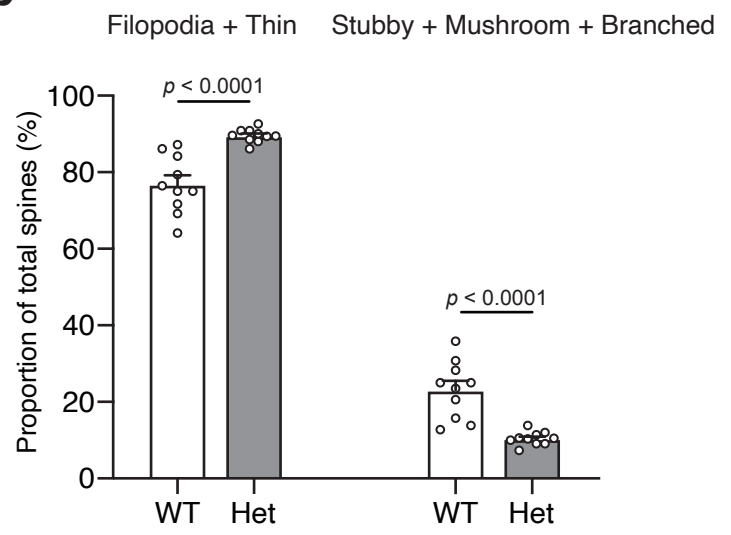
**a****b****Figure S4**



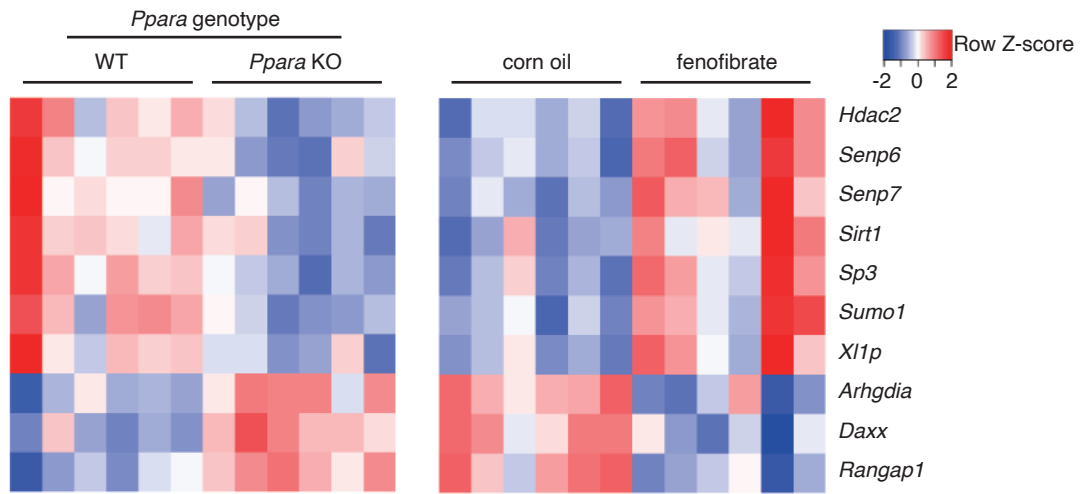
**Figure S5**



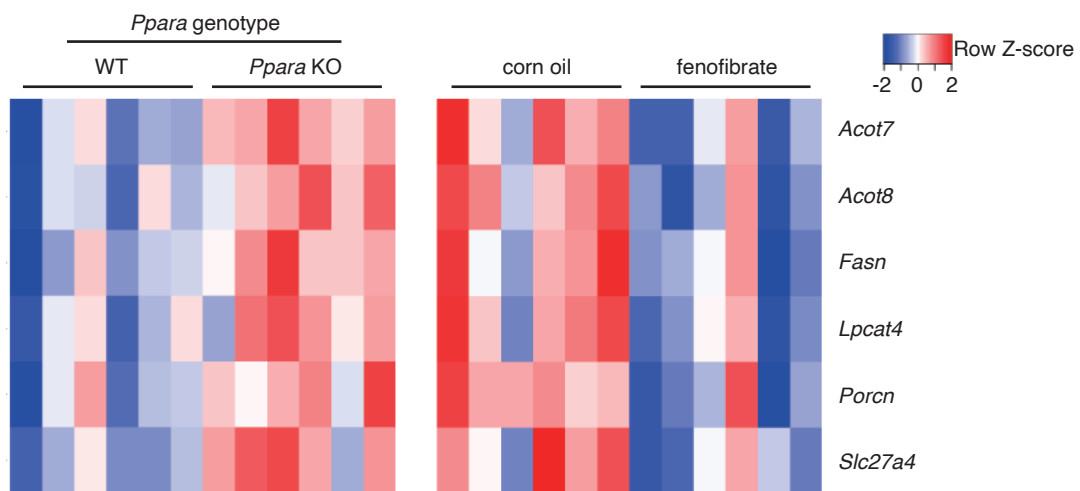
**Figure S6**

**a****b****Figure S7**

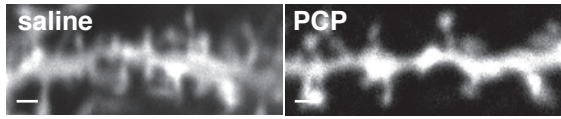
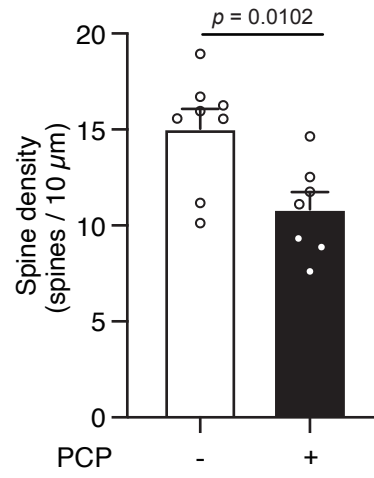
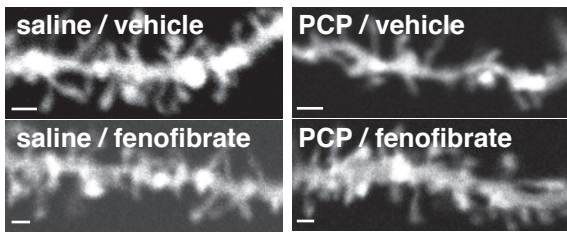
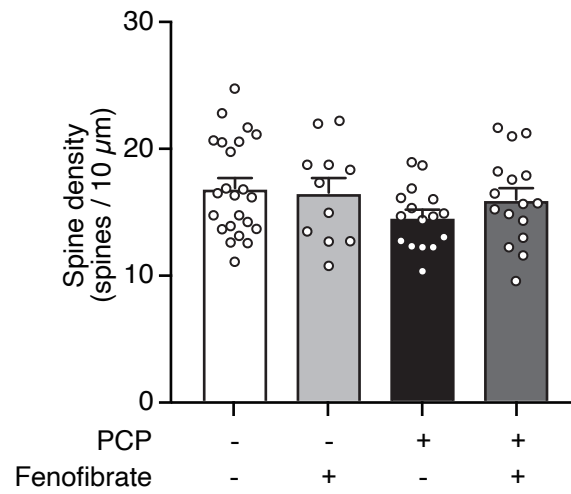
**a** Sumoylation pathway



**b** Stearate Biosynthesis



**Figure S8**

**a****b****c****d****Figure S9**